biomedicines

MDPI

Article

Platelets Induce Cell Apoptosis of Cardiac Cells via FasL after Acute Myocardial Infarction

Kim J. Krott [1,†], Friedrich Reusswig [1,†], Matthias Dille [1], Evelyn Krüger [1], Simone Gorressen [2], Saoussen Karray [3], Amin Polzin [4], Malte Kelm [4], Jens W. Fischer [2] and Margitta Elvers [1,*]

1 Department of Vascular and Endovascular Surgery, Experimental Vascular Medicine, Medical Center, Heinrich-Heine-University, 40225 Düsseldorf, Germany; kim-juergen.krott@med.uni-duesseldorf.de (K.J.K.); friedrich.reusswig@uni-mainz.de (F.R.); matthiasachim.dille@med.uni-duesseldorf.de (M.D.); evelyn_krueger@gmx.de (E.K.)
2 Institute for Pharmacology and Clinical Pharmacology, Heinrich-Heine University, 40225 Düsseldorf, Germany; simone.gorressen@med.uni-duesseldorf.de (S.G.); jefis001@hhu.de (J.W.F.)
3 INSERM U976, Université de Paris, F-7510 Paris, France; saoussenkarray@yahoo.fr
4 Department of Cardiology, Pulmonology and Angiology, Medical Center, Heinrich-Heine University, 40225 Düsseldorf, Germany; amin.polzin@med.uni-duesseldorf.de (A.P.); malte.kelm@med.uni-duesseldorf.de (M.K.)
* Correspondence: margitta.elvers@med.uni-duesseldorf.de; Tel.: +49-211-8108851
† These authors contributed equally to this work.

Abstract: Acute myocardial infarction (AMI) is one of the leading causes of death worldwide. Cell apoptosis in the myocardium plays an important role in ischemia and reperfusion (I/R) injury, leading to cardiac damage and dysfunction. Platelets are major players in hemostasis and play a crucial role in vessel occlusion, inflammation, and cardiac remodeling after I/R. Here, we studied the impact of platelets on cell apoptosis in the myocardium using a close-chest mouse model of AMI. We found caspase-3-positive resident cardiac cells, while leukocytes were negative for caspase-3. Using two different mouse models of thrombocytopenia, we detected a significant reduction in caspase-3 positive cells in the infarct border zone after I/R injury. Further, we identified platelet FasL to induce cell apoptosis via the extrinsic pathway of Fas receptor activation of target cells. Mechanistically, hypoxia triggers platelet adhesion to FasR, suggesting that platelet-induced apoptosis is elevated after I/R. Platelet-specific FasL knock-out mice showed reduced *Bax* and *Bcl2* expression, suggesting that platelets modulate the intrinsic and extrinsic pathways of apoptosis, leading to reduced infarct size after myocardial I/R injury. Thus, a new mechanism for how platelets contribute to tissue homeostasis after AMI was identified that should be validated in patients soon.

Keywords: platelets; myocardial infarction; apoptosis; cardiomyocytes; Fas ligand

Citation: Krott, K.J.; Reusswig, F.; Dille, M.; Krüger, E.; Gorressen, S.; Karray, S.; Polzin, A.; Kelm, M.; Fischer, J.W.; Elvers, M. Platelets Induce Cell Apoptosis of Cardiac Cells via FasL after Acute Myocardial Infarction. *Biomedicines* **2024**, *12*, 1077. https://doi.org/10.3390/biomedicines12051077

Academic Editors: Régis Guieu and Dong Wang

Received: 20 March 2024
Revised: 2 May 2024
Accepted: 8 May 2024
Published: 13 May 2024

1. Introduction

Ischemia and reperfusion (I/R) injury induces lethal injury to cardiomyocytes during acute myocardial infarction. There is growing evidence for cell apoptosis to play a major role in myocardial I/R injury. Extrinsic and intrinsic pathways of cell death might play a role in I/R-induced cell apoptosis, including mitochondria and cell death receptor FasR [1,2]. In contrast to necrosis, apoptosis is an active, highly regulated, and energy-requiring process of cell death occurring in the infarct core [3]. Apoptosis is induced when ligands such as Fas ligand (FasL) bound to cell-surface death receptors such as Fas (the extrinsic pathway) or when Bcl2-family pro-apoptotic proteins cause the permeabilization of the mitochondrial outer membrane (the intrinsic pathway) [4]. Both pathways merge in the activation of the caspase protease family, thereby inducing cell death by activating initiator caspases, which then activate executioner caspases, leading to the dismantling of the cell by degrading proteins indiscriminately [5].

Apoptosis after acute myocardial infarction (AMI) has been analyzed by many groups in recent years. They found that apoptosis is the major form of myocardial damage induced by coronary artery occlusion and followed by necrosis. Furthermore, apoptosis takes place at early (acute) and later (7 days) time points while necrosis peaks at 24 h post-I/R [3]. Early and late occurrence of apoptosis after AMI has also been demonstrated in humans. Using single-photon emission computed tomography, Hofstra and colleagues confirmed the presence of apoptosis early during AMI in patients [6]. Interestingly, a higher rate of apoptosis in the remote region was associated with adverse remodeling after AMI [7]. In addition, other mechanisms such as necrosis and autophagy might play a role in cardiac damage after AMI [8–10]. Thus, inhibitors of these pathways have been shown to be cardioprotective [11].

Platelets are anuclear blood cells with a strong impact on hemostasis and thrombosis. At sites of vascular damage, platelets adhere and accumulate to restore tissue integrity and avoid massive blood loss. However, uncontrolled platelet activation at sites of atherosclerotic plaque rupture is an important factor in ischemic events, as observed in patients with AMI [12]. According to the World Health Organization (WHO), ischemic heart diseases are still the global leading cause of death. Obstructed coronary vessels are re-canalized by percutaneous coronary intervention (PCI) that often leads to I/R injury, which can cause additional cardiac damage in patients with AMI [13,14].

Different knock-out or blocking strategies in experimental mice and rats, as well as human studies, revealed a significant contribution of platelets to coronary thrombosis, acute inflammation, and cardiac damage after AMI [15–22]. Recently, we have shown that elevated platelet activation after AMI contributes to I/R injury in patients and mice [19]. Enhanced platelet activation leads to the migration of platelets into the infarct border zone in the left ventricle (LV), where platelets might interact with resident cardiac cells. This allows platelets to modulate cardiac remodeling besides their role in acute inflammation by interacting with fibroblasts after AMI.

However, a role for platelets in cell apoptosis has been described recently [23]. Activated platelets induce cell apoptosis in murine neuronal cells, human neuroblastoma cells, and mouse embryonic fibroblasts by the exposure of FasL at the platelet surface. Consequently, platelet depletion resulted in reduced apoptosis in an experimental mouse model of stroke [23]. However, nothing is known about the impact of platelets on cell death after AMI.

In this study, we analyzed the capacity of platelets to substantially impact cell survival in the infarct border zone after myocardial ischemia and reperfusion. Our results provide strong evidence for platelets to induce apoptosis of resident cardiac cells in the LV via the intrinsic and extrinsic pathways, as shown by mitochondrial and FasL-induced mechanisms.

2. Materials and Methods

2.1. Animals

The animal experiments were conducted following the guidelines established by the European Parliament for the ethical use of live animals in scientific research and in compliance with German legislation concerning animal welfare. Approval for the experimental protocol was obtained from both the Heinrich Heine University Animal Care Committee and the district government of North-Rhine-Westphalia (LANUV; NRW) under Permit Numbers AZ84-02.04.2015.A558 (approval date: 26 September 2016), AZ81-02.04.2019.A270 (approval date 6 December 2019) and AZ81-02.04.2017.A440 (approval date: 23 November 2018). Wildtype (C57BL/6J) mice were purchased from Janvier (Le Genest-Saint-Isle, France).

Wildtype mice were used for induction of thrombocytopenia. Platelet depletion was initiated by administering a GPIbα antibody (No #R300, Emfret, Eibelstadt, Germany) or the corresponding IgG-control antibody (Order No #C301, Emfret, Eibelstadt, Germany) 24 h before ligating the left anterior descending coronary artery (LAD). Platelet depletion, general blood cell counts, and isolated platelet counts at various time points after ischemia/reperfusion (I/R) were monitored using the automated hematology analyzer Sysmex (Sysmex Corporation, Kobe, Japan) as already described.

Furthermore, a C57BL/6-FasL-floxed mouse strain (Inserm, Paris, France) was crossbred with the PF4-Cre recombinase-expressing mouse strain (C57BL/6-Tg(PF4-cre)Q3Rsko/J; The Jackson Laboratory, Farmington, CT, USA) to facilitate the specific knock-out of genes in megakaryocytes and platelets. Wildtype littermates corresponding to the strains were bred from parental pairs and genotyped via PCR analysis. In addition, mice with genetically induced thrombocytopenia were used ($Mpl^{-/-}$ mice). These mice with a null mutation in the thrombopoietin (TPO) receptor c-Mpl are deficient in megakaryocytes and display severe thrombocytopenia [24]. These mice were already analyzed in a mouse model of AMI recently [19].

For surgical procedures, mice were anesthetized via intraperitoneal injection with Ketamine (100 mg/mL, Ketaset, Zoetis, Malakoff, France) and Xylazine (20 mg/mL, WDT, Ulft, The Netherlands). Euthanasia was performed by cervical dislocation.

2.2. Experimental Model of Acute Myocardial Infarction (AMI) and Reperfusion in Mice

In order to mitigate surgical trauma and subsequent inflammatory reactions resulting from intervention and antibody injection following ischemia/reperfusion (I/R), a closed-chest model of reperfused myocardial infarction was employed [25]. Male mice aged 10 to 12 weeks were subjected to anesthesia via intraperitoneal injection of a solution containing Ketamine (90 mg/kg body weight) and Xylazine (10 mg/kg body weight). Upon successful induction of anesthesia, the left anterior descending artery (LAD) was ligated for 60 min to induce myocardial infarction (MI) three days post-instrumentation. Coronary occlusion was achieved by gradually tightening the applied suture until ST-elevation appeared on the electrocardiogram (ECG). Reperfusion was confirmed by the resolution of ST-elevation. After 24 h of reperfusion, hearts were excised and stained with TTC/Evans Blue solution to delineate the damaged area, distinguishing between the area at risk (ischemic area) and the infarcted area. The ratios of these distinct areas were digitally quantified using video planimetry. Left ventricular function post-MI was assessed via echocardiography at various time points after I/R (1 d, 5 d, and 21 d), utilizing a Vevo 2100 ultrasound machine (VisualSonics Inc., Bothell, WA, USA) to measure parameters including ejection fraction (%), cardiac output (mL/min), fractional shortening (%), and stroke volume (µL), with corresponding software.

2.3. Experiments with Human Blood and Study Populations

The experiments involving human blood were reviewed and approved by the Ethics Committee of Heinrich-Heine-University, adhering to the principles of the Declaration of Helsinki. Written consent was obtained from all participants before their involvement in the study.

In general, fresh citrate-anticoagulated blood (105 mM Na_3 citrate, Becton Dickinson, Franklin Lakes, NJ, USA) was collected from healthy volunteers aged 18 to 70 years in the Blood Donation Center at the University Hospital Düsseldorf for experiments under hypoxic conditions.

For the ST-elevation (STEMI) patient cohort, eligible patients admitted to the University Hospital Düsseldorf were screened for inclusion and exclusion criteria as already described [19]. Briefly, inclusion criteria comprised STEMI or chronic coronary syndrome (CCS) within existing coronary artery disease (CAD). Exclusion criteria included a palliative situation (life expectancy less than 8 weeks), pregnancy, cognitive impairment, dementia, severe chronic kidney disease (stage 3b-5), severe liver dysfunction, and platelet disorders. To mitigate potential biases, patients' characteristics were compared between groups.

Eligible patients were informed about the content of the study and asked to voluntarily participate. Written consent was obtained from all patients. The study is approved by the Heinrich-Heine University Düsseldorf ethics committee. Blood sampling was conducted directly at presentation with ST-elevation myocardial infarction in the chest pain unit before percutaneous coronary intervention. Patients were pretreated with acetylsalicylic acid by the emergency doctor before blood sampling. P2Y12 inhibition was initiated before proceeding to percutaneous coronary intervention. Therefore, patients were P2Y12 naïve at the time point of blood sampling.

To measure sFasL in the Plasma of STEMI patients, blood samples were collected from 30 STEMI and 18 CCS patients using 2.7 mL 0.1 M sodium citrate tubes (BD Vacutainer®, Becton Dickinson, Franklin Lakes, NJ, USA) and promptly centrifuged to isolate plasma samples for sFasL analysis.

2.4. Human Platelet Preparation

Human blood fresh citrate-anticoagulated blood (105 mM Na_3-citrate, BD-Vacutainer®; Becton, Dickinson, and company) was collected and centrifuged at 200× *g* for 10 min without brake. The upper phase consisting of the platelet-rich plasma (PRP) was carefully transferred into phosphate-buffered saline (PBS) pH 6.5 containing apyrase (2.5 U/mL) and 1 μM PGE_1. The tubes were centrifuged at 1000× *g* for 6 min, and the obtained pellet was resuspended in Tyrode's buffer (137 mM NaCl, 2.8 mM KCl, 12 mM $NaHCO_3$, 0.4 mM NaH_2PO_4, 5.5 mM glucose, pH 6.5). The final cell count was measured by a hematology analyzer (Sysmex KX-21N, Norderstedt, Germany) and adjusted according to the requirements of the experiment.

2.5. Platelet Adhesion to Immobilized Fas Receptor Protein

Adhesion experiments on immobilized FasR protein were performed with isolated human platelets. Isolated platelets were pre-incubated for 30 min in HEPES buffer (10 mM HEPES; 150 mM NaCl; 10 mM D-Glucose; 1 mM $MgCl_2$; 5 mM KCl; pH 7.4) under normoxic (21% O_2) or hypoxic (2% O_2) conditions in the Whitley H35 HEPA Hypoxystation. Glass coverslips (24 × 60 mm) were coated with human recombinant Fas protein (50 μg/mL, Sino Biological) at a defined area (10 × 10 mm); incubated in humidity chambers at 4 °C overnight. Coverslips were blocked with 1% BSA for at least 1 h at RT. Resting or ADP (10 μM)-stimulated platelets (4 × 10^3/μL) were pretreated with the inhibitor hDcR3 (10 μg/mL, recombinant human decoy receptor 3 protein, R&D Systems, Minneapolis, MN, USA) for 10 min and then allowed to adhere to the coated coverslips for 60 min at RT under normoxic or hypoxic conditions. IgG-Fc (10 μg/mL, R&D Systems) peptide served as control. Afterward, coverslips were rinsed two times with PBS to wash off unbound platelets. Adherent cells were fixated immediately with 4% paraformaldehyde (PFA) and covered with the mounting medium (Aquatex®). Five DIC images from different areas were taken (platelets: 400-fold total magnification; Axio Observer.D1, Carl Zeiss, Jena, Germany). The total number of adherent platelets was counted using ImageJ-win64 software.

2.6. Flow Cytometric Analysis of Blood Cells

To analyze Fas-Ligand (FasL) and PS exposure on the platelet surface, the expression was measured via fluorescence-based flow cytometry. CD42b was used as platelet platelet-specific marker in all experiments.

For detection of the PS exposure, Cy™5 AnnexinV (BD Biosciences; San Diego, CA, USA) staining was conducted while binding buffer (10 mM Hepes, 140 mM NaCl, 2.5 mM $CaCl_2$, pH 7.4) was used instead of PBS. FasL exposition and PS exposure were measured on platelets ($CD42b^+$ population) in washed whole blood 24 h after MI. Samples were incubated with Annexin Cy^{TM5} or PE-labeled FasL antibody (CD178-PE, NOK1, Biolegend, San Diego, CA, USA) for 15 min at RT. Reactions were stopped by adding 500 µL PBS or AnnexinV binding puffer, respectively, and measured at a FASCalibur (BD). MFI of FasL was measured in the platelet population, representing the FasL exposition on platelets.

For PS exposure and FasL externalization analysis under normoxic (21% O_2) or hypoxic (2% O_2) conditions, isolated human platelets were pre-incubated for 30 min under these conditions in HEPES buffer (10 mM HEPES, 150 mM NaCl, 10 mM D-Glucose, 1 mM $MgCl_2$, 5 mM KCl, pH 7.4) in the Whitley H35 HEPA Hypoxystation. Resting or collagen-related peptide (CRP)-activated platelets were labeled and analyzed as described before. CRP is a collagen-like synthetic peptide with the sequence, {[Gly-Cys-Hyp-(Gly-Pro-Hyp)$_{10}$-Gly-Cys-Hyp-Gly-amide]$_3$} and is a highly potent platelet agonist, which activates the major collagen receptor GPVI at the surface of platelets. Like collagen, CRP has a tertiary (triple-helical) and quaternary (polymeric) structure to activate platelets.

2.7. Enzyme-Linked Immunosorbent Assay (ELISA)

For quantification of soluble FasL in the plasma of mice, heparinized blood was centrifuged for 10 min for 650× *g* to collect the plasma. The amount of soluble FasL was measured by an ELISA Kit from My Biosource, San Diego, CA, USA, following the manufacturer's protocol.

For the detection of sFasL in STEMI patients, plasma was collected in EDTA tubes. Samples were centrifuged at 1000× *g* for 30 min before proceeding to ELISA (Human FAS Ligand ELISA Kit—CD95L–Abcam-ab100515).

2.8. Immunohistochemistry of Cardiac Sections

At different time points after ischemia/reperfusion, hearts were flushed with cold heparin solution (20 U/mL, Roche, Basel, Switzerland), removed, paraffin-embedded and cut into 5 µm sections using an automatic microtome (Microm HM355, Thermo Fisher Scientific, Dreieich, Germany). Prior to staining, all sections were deparaffinized and hydrated. For antigen unmasking, the tissue sections were heated at 300 W in citrate buffer (pH 6.0) for 10 min.

For fluorescence staining of apoptotic cells in the LV, the following antibodies were used: Cleaved caspase-3 (Casp-3, #9661, Cell Signaling (Danvers, MA, USA), 1:50), vimentin (#PA5-142829, Invitrogen, 1:50), troponin (#MA5-12960, Invitrogen (Carlsbad, CA, USA), 1:50) and CD45 (#55307, Cell Signaling, 1:100). The heart tissue sections were blocked with DPBS (containing 0.3% Triton x-100 and 5% goat serum) for 1 h at RT. After overnight incubation with the respective primary antibodies at 4 °C, the sections were stained with a highly cross-adsorbed Alexa Fluor™ Plus 555 conjugated secondary antibody (#A32794, Invitrogen™, 1:200) and Alexa Fluor™ 647 conjugated secondary antibody (#A21247, Invitrogen™, 1:200) for 1 h at RT. In control experiments, the first antibodies were omitted, and the sections were only stained with secondary antibodies. For analyzing apoptosis in thrombocytopenic or FasL knock-out mice after myocardial infarction, paraffin-embedded heart sections were immune-stained with cleaved Caspase-3 as primary antibody, followed by labeling with streptavidin biotin/horseradish peroxidase (LSAB2 System HRP, Dako, Santa Clara, CA, USA) and Diaminobenzidine (DAB)—Chromogen (Dako, Santa Clara, CA, USA), performed as standard protocol.

To visualize nuclei, all tissue sections were stained with DAPI (4′,6-Diamidine-2′-phenylindole dihydrochloride, #10236276001, Roche, 1:3000). Images were taken with a confocal microscope from Zeiss (LSM 880 Airyscan, Jena, Germany).

2.9. Quantitative Real-Time Polymerase Chain Reaction (qRT-PCR)

To evaluate the endogenous expression levels of Bax and *Bcl2*, isolated total RNA from the LV 24 h post-myocardial infarction was utilized. LVs were separated and homogenized in Trizol using the Precellys tissue homogenizer (Precellys 24-Dual Homogenizer, Bertin, Frankfurt am Main, Germany) for 30 s at 5000 rpm. The supernatant was collected, chloroform was added, and RNA isolation was carried out using an RNAeasy Mini Kit (Qiagen, Hilden, Germany), following the manufacturer's instructions. Following reverse transcription, quantitative PCR amplification was conducted using the following oligonucleotide primers:

Bax	forward 5′TGAAGACAGGGGCCTTTTTG 3′;	reverse 5′AATTCGCCGGAGACACTCG 3′;
Bcl2	forward 5′GACAAGGAGATGCAGGTATTGG 3′;	reverse 5′TCCCGTAGAGACCACAAAAGT 3′;
Gapdh	forward 5′GGTGAAGGCGGTGTGAACG 3′;	reverse 5′CTCGCTCCTGGAAGATGGTG 3′

Quantitative real-time PCR was performed using Fast Sybr Green Master Mix (Thermo Fischer Scientific, Waltham, MA, USA) according to a standard protocol. The expression levels of *Bax* or *Bcl2* were normalized to glyceraldehyde-3-phosphate dehydrogenase (Gapdh) RNA expression levels from naïve control mice.

2.10. Statistical Analysis

The experiments were conducted a minimum of three times, with 'n' representing each individual animal. Results are expressed as means ± SEM. Statistical analysis was conducted using GraphPad Prism 10.0 software (GraphPad Software, Inc., San Diego, CA, USA). Statistical tests included *t*-tests and one-way or two-way ANOVA, with significance set at $p < 0.05$. In all figures, significance levels were denoted as * $p < 0.05$, ** $p < 0.01$, and *** $p < 0.001$.

3. Results

3.1. Ischemia and Reperfusion-Induced Cell Apoptosis of Resident Cardiac Cells in the Infarct Border Zone after AMI in Mice

After acute myocardial infarction, ischemia and reperfusion injury lead to cell apoptosis in the myocardium [26]. To identify cells in the myocardium that are affected by cell apoptosis, we first performed a histological analysis using different cellular markers to stain cardiomyocytes (troponin), cardiac fibroblasts (vimentin) and leukocytes (CD45) that have been migrated into the infarct border zone. As shown in Figure 1, we detected caspase-3 positive cardiomyocytes (Figure 1A,B) and caspase-3 positive fibroblasts (Figure 1C,D) in the infarct border zone of mice that underwent acute myocardial infarction using cardiac sections of the LV at day 5 post-I/R. However, the analysis of CD45-positive leukocytes revealed that these cells are not affected by apoptosis (Figure 1E,F). Thus, only resident cardiac cells but not migrated inflammatory cells showed signs of apoptosis as detected by caspase-3 positive cardiomyocytes and fibroblasts.

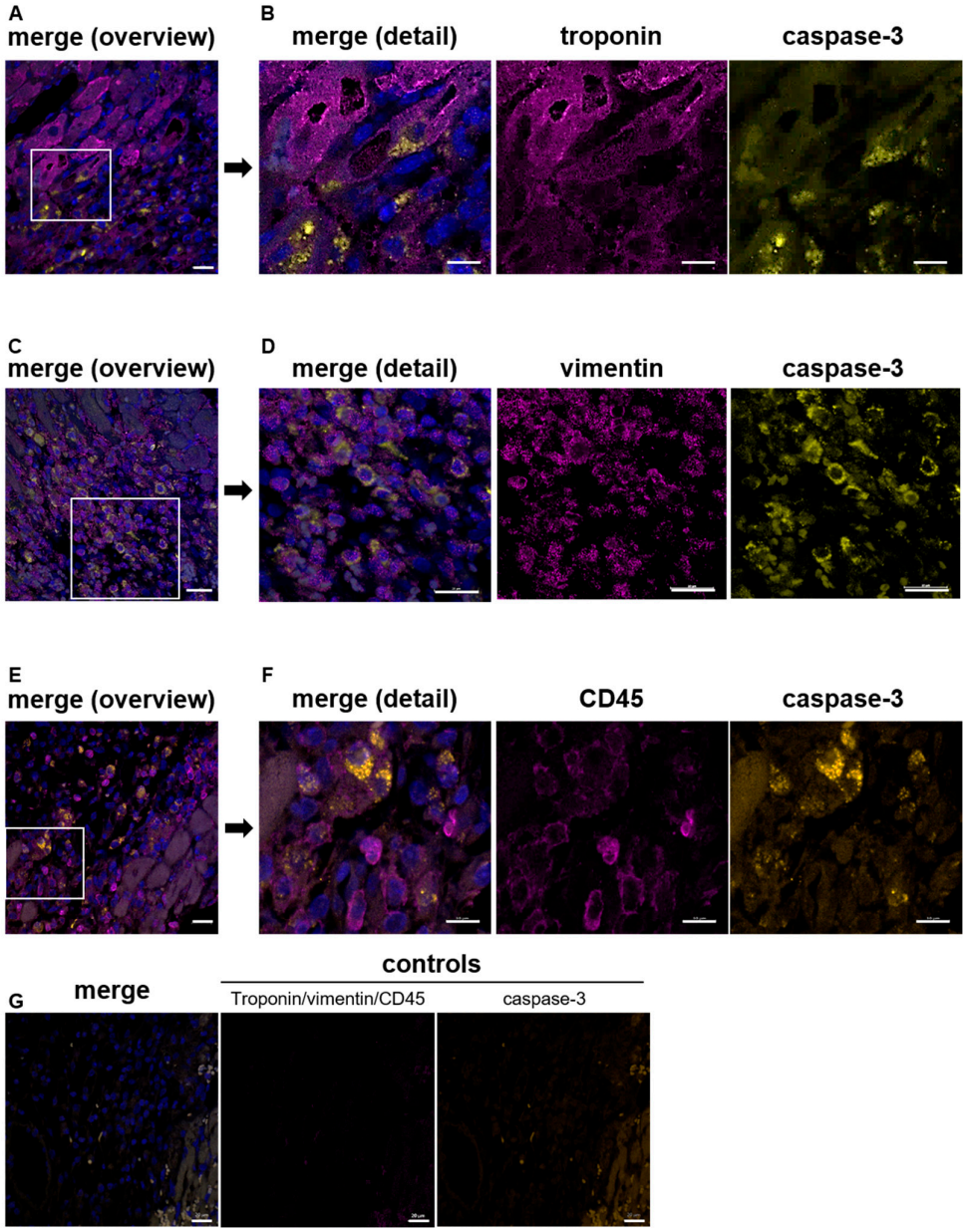

Figure 1. Ischemia and reperfusion injury lead to apoptosis of resident cardiac cells in the infarct border zone 5 days after AMI in mice. White boxes in (**A**,**C**,**E**) indicate zoom-in area shown in (**B**,**D**,**F**), respectively (**A**,**B**) Representative images of cardiac sections from the infarct border zone 5 days after I/R stained for troponin as a marker for cardiomyocytes and caspase-3, (**A**) overview, (**B**) section from A to show details of caspase-3 positive cardiomyocytes; n = 4. (**C**,**D**) Caspase-3 positive cardiac fibroblasts in the infarct border zone were detected 5 days post-AMI. (**C**) Overview, (**D**) details of vimentin stained fibroblasts; n = 3–5. (**E**,**F**) CD45-stained leukocytes show no signs of apoptosis using cardiac sections of the infarct border zone 24 h post-I/R. (**E**) Overview and details (**F**) of CD45 stained leukocytes and caspase-3 positive cells were shown; n = 4–6. (**G**) Controls of troponin/vimentin/CD45 and caspase-3 staining were shown using PBS and the appropriate secondary antibody (the same secondary antibody was used for troponin, vimentin, and CD45). In all samples, DAPI was used to stain nuclei in cardiac sections. Scale bar, (**A**,**C**,**F**,**G**) = 20 μm, (**B**,**D**) = 10 μM, (**E**) = 30 μM.

3.2. Reduced Cardiac Cell Apoptosis in Thrombocytopenic Mice after Acute Myocardial Infarction

Cell apoptosis plays a crucial role in LV remodeling after AMI [27]. Several extracellular signals regulate apoptosis in cardiomyocytes, which ends up in the activation of

caspase-3 [28]. To analyze if platelets play a role in cell apoptosis in the infarct border zone after I/R, we analyzed platelet-depleted and MPL knock-out mice that suffer from thrombocytopenia. First, we determined the number of caspase-3 positive cells in the infarct border zone of thrombocytopenic mice by histologic analysis of infarcted heart sections. As shown in Figure 2A, a significant reduction in apoptotic cells has been observed in mice with almost no platelets (platelet-depleted mice) and in MPL knock-out mice with platelet counts of ~10% [19]. To investigate which mechanisms play a role in platelet-induced cell apoptosis post-AMI, we first investigated mitochondria-dependent apoptosis via the intrinsic pathway. A lower expression of the apoptosis-associated gene *Bax* was found in the LV of platelet-depleted mice after 24 h of reperfusion (Figure 2B), while non-depleted control mice showed an enhanced *Bax* gene expression due to ischemia and reperfusion injury (Figure 2B). In line with enhanced *Bax* expression, an increase in gene expression of the anti-apoptotic *Bcl2* in the LV was observed in mice where platelets have been depleted after AMI, while no differences were observed in IgG control mice (Figure 2C). In contrast, chronic thrombocytopenic MPL knock-out mice displayed no differences in *Bax* and *Bcl2* gene expression in the LV 24 h after ischemia and reperfusion injury (Figure 2B,C).

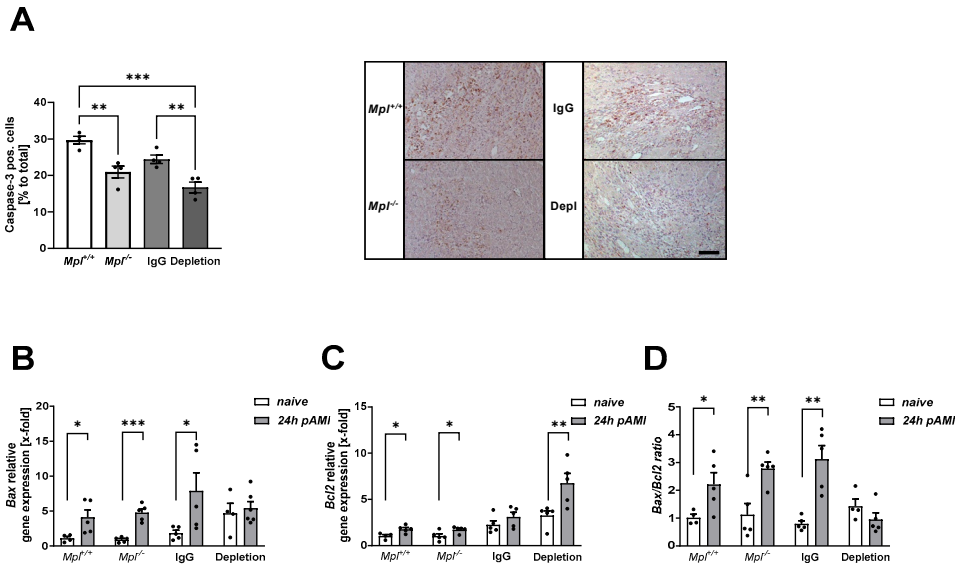

Figure 2. Reduced cardiac cell apoptosis in thrombocytopenic mice after acute myocardial infarction. (**A**) Quantification (**left panel**) and representative images (**right panel**) of caspase-3 positive cells in the infarct border zone of platelet depleted and Mpl deficient mice compared to controls 5 days after AMI; n = 4. (**B**–**D**) mRNA analysis of pro-apoptotic *Bax* (**B**) and anti-apoptotic *Bcl2* (**C**) genes in the LV (left ventricle) of thrombocytopenic naïve mice and 24 h post-AMI compared to respective control mice; n = 4–6 (**B**); n = 4–6 (**C**). (**D**) Cell death switch as shown by the *Bax*/*Bcl2* ratio. Scale bar = 50 µm. Data are presented as means ± SEM. Statistical analyses were carried out by (**A**) two-way ANOVA followed by Sidak post hoc and (**B**,**C**) multiple *t*-test. * $p < 0.05$, ** $p < 0.01$, *** $p < 0.001$). Scale bar = 50 µm.

3.3. Increased Adhesion of Platelets to Immobilized Fas Receptor under Hypoxic Conditions

Besides cell apoptosis via the intrinsic pathway, cells can undergo apoptosis by the extrinsic pathway via TNF or FasL [29]. The FasL-FasR plays an important role in the extrinsic pathway of cell apoptosis [30]. Shedding of the FasL to its soluble form (sFasL) is associated with the loss of its apoptotic function because sFasL blocks the activity of FasR [31]. Platelets are known to expose FasL at the membrane that is associated with platelet-RBC interaction [32] and platelet-induced cell apoptosis [23]. Therefore, we next analyzed the impact of platelet FasL binding to FasR under hypoxic conditions. As shown in Figure 3A, platelets adhere to immobilized recombinant FasR under physiological

oxygen levels. However, hypoxic conditions induced increased adhesion of platelets to immobilized FasR.

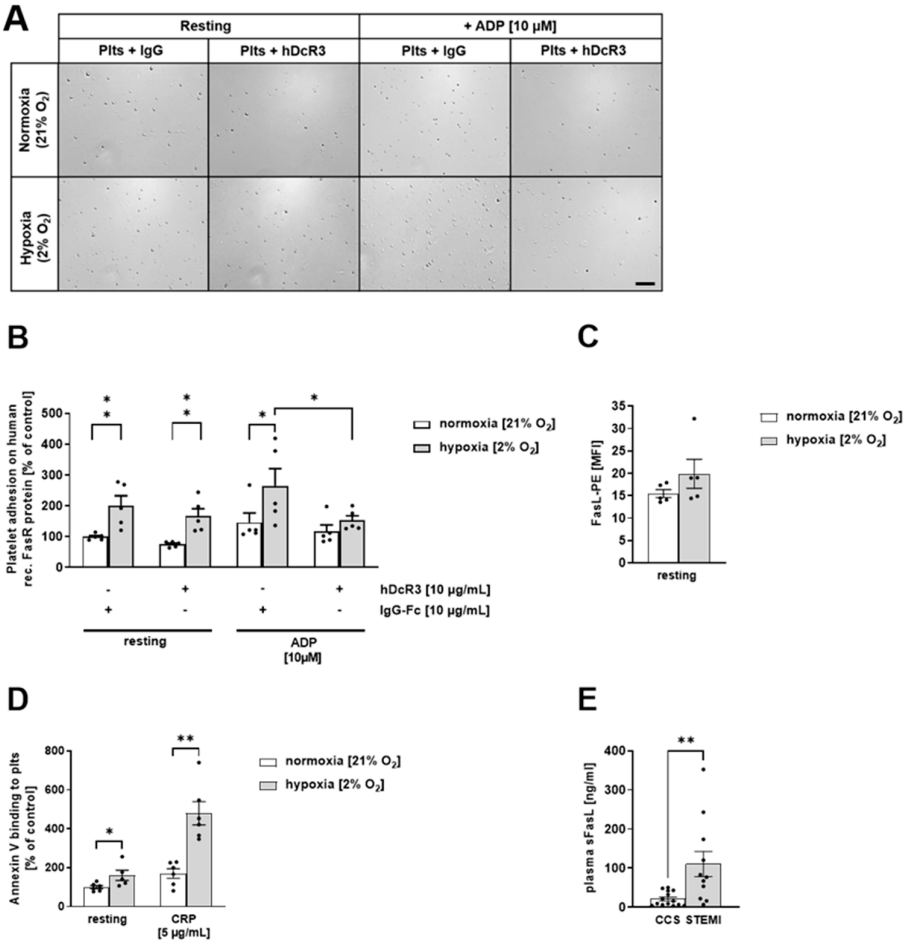

Figure 3. Increased adhesion of platelets to immobilized FasR under hypoxic conditions. (**A**) Representative images and (**B**) Quantification of adherent resting and ADP [10 µM]-stimulated human platelets to immobilized human recombinant FasR protein (50 µg/mL) under normoxic (21% O_2) or hypoxic (2% O_2) conditions (n = 4–6). (**C**) Externalization of FasL on the surface human platelet determined by flow cytometry (n = 5). (**D**) Annexin V binding to resting and CRP [5 µg/mL]-stimulated human platelets under normoxic (21% O_2) or hypoxic (2% O_2) conditions (n = 5–6) determined by flow cytometry. (**E**) Soluble (s)FasL plasma level (in ng/mL) from patients with coronary heart disease (CHD) compared to ST-elevation myocardial infarction (STEMI)-patients (n = 11–14). Scale bar = 50 µm (missing). Data are presented as means ± SEM. Statistical analyses were carried out by (**B**) two-way ANOVA followed by Sidak post hoc; (**C**,**E**) by two-tailed unpaired Student's *t*-test, and (**D**) multiple t-test. * $p < 0.05$, ** $p < 0.01$.

Platelet activation with ADP where the FasL was blocked by hDcR3 resulted in reduced platelet adhesion compared to IgG-Fc controls (Figure 3A,B), suggesting that the increase in platelet adhesion upon stimulation with ADP under hypoxic conditions is mediated by FasL binding of platelets to recombinant FasR. FasL exposure of platelets was enhanced by trend under hypoxic conditions (Figure 3C), while Annexin-V binding was significantly enhanced under hypoxia, as shown by the analysis of resting and CRP-stimulated platelets (Figure 3D). Further evidence for FasL to be involved in I/R injury after AMI was provided by data from STEMI patients showing elevated plasma levels of sFasL compared to the CCS control group (Figure 3E).

Consequently, we analyzed FasL exposure at the surface of platelets after 6 h and 24 h of ischemia and reperfusion (Figure 4A). The exposure of FasL at the platelet membrane

was significantly reduced 6 h and 24 h after I/R injury in wildtype C57BL/6 mice. In line with reduced platelet FasL exposure, we detected elevated plasma levels of sFasL in these mice 24 h and 5 days after AMI, suggesting that I/R injury leads to enhanced shedding of FasL after AMI (Figure 4B).

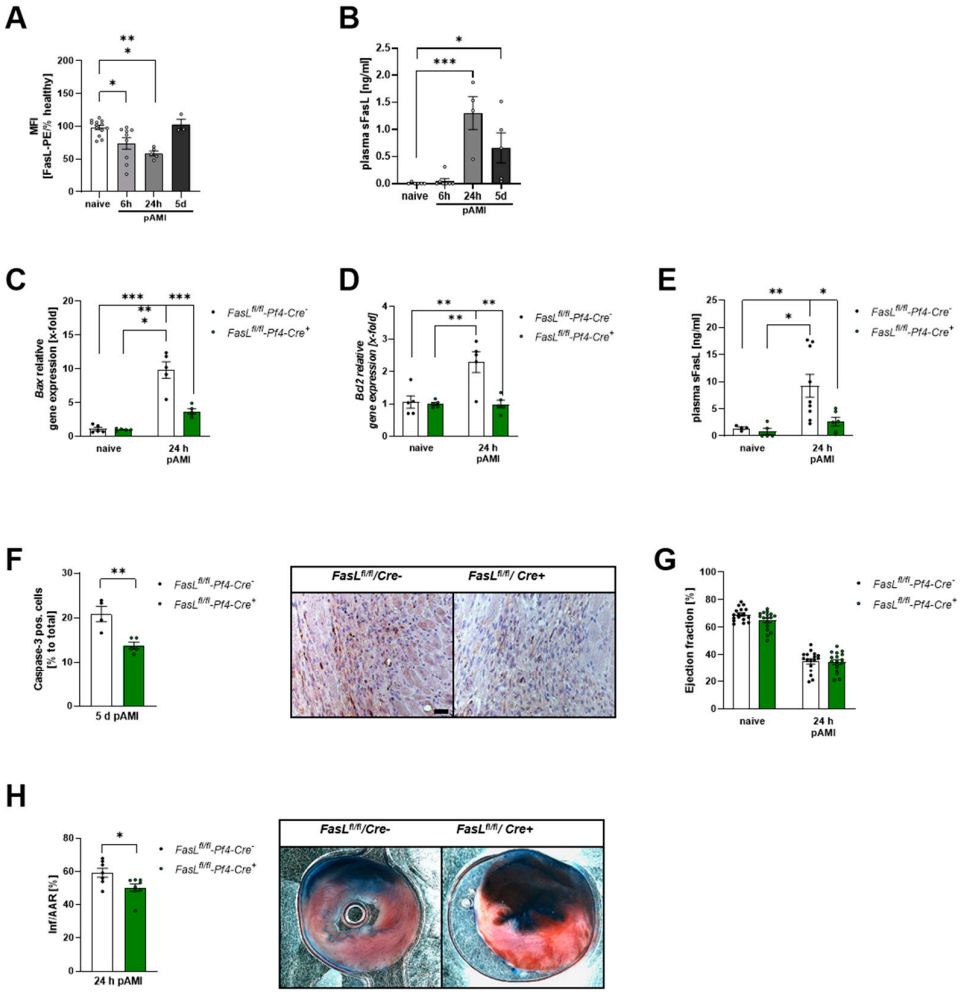

Figure 4. Genetic deficiency of platelet-specific FasL leads to reduced apoptosis post-AMI. (**A**) FasL exposure at the platelet surface of naïve mice and 6 h, 24 h, and 5 days post-AMI; n = 13. (**B**) Plasma levels of soluble FasL (sFasL) in naïve mice and 6 h, 24 h and 5 days post-AMI; n = 5–7. (**C**,**D**) mRNA analysis of pro-apoptotic *Bax* (**C**) and anti-apoptotic *Bcl2* (**D**) genes in the LV of *FasL*$^{fl/fl}$*-Pf4-Cre*− and *FasL*$^{fl/fl}$*-Pf4-Cre*+ naïve mice and 24 h post-AMI; n = 5. (**E**) Plasma levels of sFasL in *FasL*$^{fl/fl}$*-Pf4-Cre*− and *FasL*$^{fl/fl}$*-Pf4-Cre*+ naïve mice and 24 h post-AMI; n = 4–9. (**F**) Quantification (**left panel**) and representative images (**right panel**) of caspase-3 positive cells in the heart of *FasL*$^{fl/fl}$*-Pf4-Cre*- and *FasL*$^{fl/fl}$*-Pf4-Cre*+ mice 5 days after AMI; n = 4–5. (**G**) Echocardiographic analysis of cardiac function by determination of ejection fraction (baseline vs. 24 h after I/R) of *FasL*$^{fl/fl}$*-Pf4-Cre*− and *FasL*$^{fl/fl}$*-Pf4-Cre*+ mice; n = 12–13. (**H**) Quantitative analysis (**left panel**) of infarct size as the percentage of the area at risk (% Inf/AAR) with representative images (**right panel**) of *FasL*$^{fl/fl}$*-Pf4-Cre*− and *FasL*$^{fl/fl}$*-Pf4-Cre*+ mice 24 h post-AMI. Blue = healthy tissue, red = the area at risk (AAR), white = infarcted area (INF); n = 7. Scale bar = 50 µm. White bars = *FasL*$^{fl/fl}$*-Pf4-Cre-; green bars* = *FasL*$^{fl/fl}$*-Pf4-Cre*+ Data are presented as means ± SEM. Statistical analyses were carried out by two-way ANOVA followed by Sidak post hoc (**A**–**E**,**G**) or by two-tailed unpaired Student's *t*-test (**F**,**H**). * $p < 0.05$, ** $p < 0.01$, *** $p < 0.001$.

3.4. Platelet FasL Exposure Mediates Cell Apoptosis in the Left Ventricle Post-AMI

According to the results shown in Figure 3, we analyzed the impact of the platelet-specific loss of FasL on cell apoptosis post-AMI using *FasL*$^{fl/fl}$*-Pf4-Cre*+ mice that do not

express FasL on the platelet surface [32]. *FasL$^{fl/fl}$-Pf4-Cre−* mice were used as wild-type controls. Accordingly, AMI induced significantly elevated *Bax* gene expression in the LV of *FasL$^{fl/fl}$-Pf4-Cre−* mice after 24 h of reperfusion compared to naïve conditions (Figure 4C). However, *FasL$^{fl/fl}$-Pf4-Cre+* mice showed only a weak increase in LV *Bax* expression compared to naïve conditions and were significantly lower compared to *FasL$^{fl/fl}$-Pf4-Cre−*. Further, AMI also induced LV *Bcl2* expression in FasL wild-type mice (Figure 4D). Similarly to *Bax* expression, *FasL$^{fl/fl}$-Pf4-Cre+* mice showed almost no upregulation of *Bcl2* expression after AMI compared to naïve mice and less *Bcl2* expression compared to *FasL$^{fl/fl}$-Pf4-Cre−* (Figure 4D). In addition, the analysis of plasma levels of sFasL in *FasL$^{fl/fl}$-Pf4-Cre−* and *FasL$^{fl/fl}$-Pf4-Cre+* post-AMI revealed a significant increase in *FasL$^{fl/fl}$-Pf4-Cre−* mice that were strongly reduced in *FasL$^{fl/fl}$-Pf4-Cre+* mice 24 h after AMI, suggesting that platelets are major contributors of sFasL plasma levels after AMI (Figure 4E). Furthermore, histological analyses revealed that the loss of platelet FasL is responsible for reduced caspase-3 activity in the LV of *FasL$^{fl/fl}$-Pf4-Cre+* mice after 5 days of reperfusion (Figure 4F). Nevertheless, the FasL-associated changes in LV apoptosis alone had no influence on heart function post-AMI (Figure 4G and Table 1). However, after 24 h of reperfusion, we detected a reduced infarct size in *FasL$^{fl/fl}$-Pf4-Cre+* mice compared to controls (Figure 4H) due to reduced cell apoptosis after ischemia and reperfusion injury.

Table 1. Different parameters of LV function and wall thickness of mice after AMI. Echocardiographic analysis was conducted to evaluate heart function and wall thickness parameters in *FasL$^{fl/fl}$-Pf4-Cre* mice following ischemia/reperfusion (I/R) injury (n = 17). Data are presented as means ± SEM. Statistical significance was determined using two-way ANOVA with Sidak's multiple comparison test. Bold *p*-Values indicate statistical significance. LVAWs = left ventricular anterior wall thickness during systole; LVAWd = left ventricular anterior wall thickness during diastole; LVPWs = left ventricular posterior wall thickness during systole; LVPWd = left ventricular posterior wall thickness during diastole. *p*-values represent a comparison between genotypes at indicated time points.

	Naive					**24 h Post-AMI**				
	FasL$^{fl/fl}$-Pf4-Cre−		***FasL$^{fl/fl}$-Pf4-Cre+***		***p-Value***	***FasL$^{fl/fl}$-Pf4-Cre−***		***FasL$^{fl/fl}$-Pf4-Cre+***		***p-Value***
	mean	***s.e.m.***	***mean***	***s.e.m.***		***mean***	***s.e.m.***	***mean***	***s.e.m.***	
systolic volume [µL]	18.83	1.10	20.45	1.59	*0.8145*	48.98	2.88	46.07	1.99	*0.5183*
diastolic volume [µL]	60.46	2.10	57.50	2.05	*0.5799*	75.42	2.78	71.50	1.89	*0.3885*
stroke volume [µL]	42.00	1.56	37.00	1.19	***0.0189***	26.44	1.42	25.43	1.07	*0.8343*
cardiac output [µL]	21.25	0.85	16.16	1.26	***0.0005***	15.17	0.78	14.76	0.73	*0.9397*
heart rate [BPM]	506.27	9.31	485.14	13.50	*0.504*	576.51	9.10	582.82	21.24	*0.9394*
fractional shortening [%]	18.13	0.87	17.74	1.12	*0.9534*	10.86	1.04	10.72	1.01	*0.9943*
LVAWd [mm]	0.58	0.02	0.61	0.01	*0.5211*	0.66	0.03	0.66	0.02	*0.9896*
LVAWs [mm]	0.82	0.03	0.85	0.02	*0.5364*	0.74	0.03	0.75	0.02	*0.9963*
LVPWd [mm]	0.64	0.02	0.64	0.02	*0.9939*	0.67	0.02	0.69	0.03	*0.701*
LVPWs [mm]	1.05	0.03	0.98	0.04	*0.4427*	0.91	0.04	0.90	0.05	*0.9723*

4. Discussion

In this study, we found that I/R injury leads to apoptosis of resident cardiac cells after AMI in mice. Platelets are one major contributor to cell apoptosis because thrombocytopenia and genetically modified mice with a loss of FasL restricted to platelets resulted in reduced cardiac cell death via the intrinsic and the extrinsic pathway of apoptosis. Mechanistically, we provide the first evidence that platelet binding to FasR is significantly elevated under hypoxic conditions, as found in AMI.

In AMI, apoptosis is a key pathological determinant since the inhibition of apoptosis has a beneficial effect in experimental studies. Thus, understanding the mechanisms that lead to apoptosis is important for therapeutic options to prevent and/or treat heart failure induced by ischemic reperfusion injury but also for diagnosis and risk stratification in patients with ischemic heart disease [3]. To date, it is still not completely understood to which extent apoptosis counts for cardiac damage because of the large differences in

reports from different groups. There might also be differences in the induction of apoptosis by ischemia and/or by reperfusion. Ischemia alone did not result in DNA laddering, a marker of apoptosis, but was observed after reperfusion, indicating that apoptosis in the myocardium is triggered upon reperfusion but does not manifest during the ischemic event. In contrast, others found that myocardial ischemia induced apoptosis when a prolonged ischemic period without any reperfusion was observed, while others detected apoptosis after brief ischemic events followed by reperfusion [9,33]. However, different studies provided evidence for the initiation of apoptosis upon ischemia as indicated by pro-apoptotic markers and caspase activation but no DNA fragmentation followed by a massive increase during reperfusion. Thus, it becomes evident that apoptosis might be fully conducted during reperfusion. The assumption that reperfusion is a trigger for apoptosis has been further strengthened by a study where inhibitors of pro-apoptotic mediators were used because reduced infarct size at early reperfusion was detected [11]. Studies in humans provided evidence for long-lasting cell apoptosis in the myocardium because they detected apoptotic cardiomyocytes in the border zone of the infarcted myocardium within hours to days of infarction [34]. On the contrary, minimal expression of proteins of the apoptosis signaling cascade in cardiomyocytes argues against a significant role of apoptosis in I/R-induced cell death [35]. This hypothesis has been reinforced by knock-out mice with cardiac-specific ablation of caspase-3 and caspase-7 that do not show beneficial effects for infarct size or LV remodeling, indicating no acute effects on myocardial I/R injury [36]. Thus, it is not surprising that overexpression of caspase in cardiomyocytes does not lead to increased apoptosis in cardiomyocytes but elevated infarct size during I/R [37]. These results together implicate that the previous observations of apoptosis in the heart are likely to have been due to apoptosis of non-cardiomyocytes [35]. This hypothesis is emphasized by the idea that apoptosis of endothelial cells and leucocytes might indirectly affect cardiomyocyte cell survival and cardiac performance [35], suggesting that anti-apoptotic strategies might still be cardio-protective. A recently published study confirmed the importance of anti-apoptotic treatments because the injection of a newly developed peptide targeting the Fas-dependent apoptotic signal at the onset of reperfusion led to strong cardio-protection in vivo by inhibiting I/R injury [38]. In line with our study using platelet-specific FasL knock-out mice, decreased infarct size was shown when the Fas-dependent apoptotic pathway was blocked with this peptide, suggesting that the FasL-FasR signaling pathway is a promising target to reduce myocardial injury after AMI. Importantly, hypoxia plays a role in FasL-FasR induced cell apoptosis because reduced oxygen supply triggers increased expression of FasR on cardiomyocytes on the one hand [39,40] and the ability of platelets to adhere to FasR on the other hand (Figure 3).

Platelets play a major role in ischemic cardiovascular disease. Beyond thrombotic complications, they modulate inflammation and cardiac remodeling [18,19]. Here, we provide strong evidence for platelets to induce cell apoptosis of resident cardiac cells via exposure to FasL. Data from Mpl deficient and platelet-depleted mice clearly show a significant contribution of platelets to cell death via apoptosis induced by the intrinsic and the extrinsic pathways. Recently, we have shown that platelets are the major source of IL-1β after I/R because IL-1β plasma levels were almost absent in platelet-depleted mice 24 h post-AMI [19]. However, IL-1β is not only a crucial acute phase cytokine important to induce the activation and secretion of IL-1β from leukocytes but is also responsible for the increase in FasL-induced caspase-3 activation as shown in hepatocytes [41]. Thus, reduced apoptosis in platelet-depleted mice after AMI might be provoked by different mechanisms such as reduced IL-1β plasma levels, reduced hypoxia, and absent platelet-FasL-induced cell apoptosis of migrated platelets in the infarct zone. Besides reduced intrinsic and mitochondrial cell death as a result of reduced hypoxia in platelet-depleted mice, we provided evidence that platelet FasL induces cell death in the infarct zone of the LV. Platelet-specific genetic deficiency of FasL led to reduced apoptosis in the LV and thus affects infarct size but not cardiac function. However, we detected a significant difference in naïve mice but not after AMI when we compared the stroke volume and cardiac output

between platelet-specific FasL knock-out mice and controls (Table 1). This implies that the decrease in cardiac function in FasL knock-out mice before and after AMI is lower than in control mice. Thus, genetic deficiency of platelet-specific FasL might lead to a chronic protective effect of left ventricular function but does not exert an acute effect because no differences between genotypes were observed 24 h after I/R.

In the past, platelet FasL has been shown to trigger cell death in murine neuronal cells and in a murine stroke model [23]. It was shown that *Bax*/*Bak*-induced mitochondrial apoptosis signaling in target cells was not required for platelet-induced cell death but increased the apoptotic response to platelet-FasL-induced Fas signaling. Here, we also found reduced *Bax* and *Bcl2* expression in the LV of mice with platelet-specific FasL ablation (Figure 4A,B). Thus, mitochondrial-induced cell death after AMI might trigger the observed platelet FasL-induced cell apoptosis in the LV. However, there might be additional mechanisms that account for reduced cell apoptosis in platelet-depleted mice after AMI because additional death receptor ligands are known to be stored and secreted by platelets such as TRAIL (Apo2-L), TWEAK (Apo3-L) and LIGHT which have the capacity to regulate apoptosis via paracrine signaling [42–44].

Mitochondria play an important role in cell apoptosis because they are the major contributors of reactive oxygen species (ROS) and the major target of ROS-induced damage. Typical characteristics of the mitochondrial apoptosis pathway are mitochondrial swelling and outer mitochondrial membrane rupture that triggers the release of pro-apoptotic factors such as cytochrome c and SMAC/Diablo from the intermembrane space into the cytosol [45]. Interestingly, chronic thrombocytopenia does not reduce mitochondrial (intrinsic) apoptosis in the myocardium of MPL knock-out mice, as shown by the unaltered expression of *Bax* and *Bcl2*. As already shown by Schleicher and colleagues, mitochondrial apoptosis signaling is not required for platelet-induced cell death [23]. Thus, the reduction in caspase-3 positive cells in the myocardium of MPL knock-out mice is the result of extrinsic apoptotic mechanisms, probably via FasL-mediated activation of FasR. However, different results of mice with chronic and acute thrombocytopenia might also be due to different platelet counts in these mice. While platelet-depleted mice represent a platelet count of <1%, we detected ~10% of platelet numbers in Mpl-deficient mice compared to controls [19]. Thus, it is tempting to speculate that differences of around 10% of platelet counts might be sufficient for alterations in mitochondria-mediated apoptosis in the myocardium.

Interestingly, the soluble form of FasL is not able to trigger apoptosis [46]. After AMI, the exposure of FasL at the platelet surface was reduced at 6 h and 24 h post-I/R, which correlates with enhanced plasma levels of FasL after AMI. However, our results clearly indicate that the majority of plasma sFasL is of platelet origin because plasma levels of sFasL are strongly reduced in platelet-specific FasL knock-out mice (*FasL*$^{fl/fl}$*-Pf4-Cre+*). Consequently, platelets might be involved in the prevention of cell apoptosis of non-resident cells in the circulation, such as leukocytes, by activation-induced shedding of the FasL from the platelet surface.

5. Conclusions

Recent findings, together with the here-presented results of platelet-induced cell apoptosis, clearly indicate the important role of platelets for cardiac function beyond occlusive ischemic damage post-AMI. Platelets support the acute inflammatory response and migrate into the infarct border zone to actively modulate cardiac remodeling and cell apoptosis and thus contribute to tissue homeostasis. These newly identified mechanisms of platelet-induced cardiac damage need to be validated in patients with AMI. This might be important to re-evaluate current anti-thrombotic/antiplatelet strategies to confirm that aspirin and P2Y12 inhibitors affect all these processes post-AMI or if there is a need to optimize the treatment of AMI patients.

Author Contributions: Conceptualization, M.E.; methodology, S.G.; validation, M.K., J.W.F. and M.E.; investigation, K.J.K., F.R., M.D., E.K. and A.P.; resources, S.K.; writing—original draft preparation, M.E., F.R. and K.J.K.; writing—review and editing, M.E.; funding acquisition, M.E. All authors have read and agreed to the published version of the manuscript.

Funding: The study was funded by the Deutsche Forschungsgemeinschaft (DFG, German Research. Foundation)—Grant number 236177352—SFB 1116, project A05 and grant number 397484323—CRC/TRR259, project A07 to M.E.

Institutional Review Board Statement: Animal studies were performed in accordance with the guidelines of the European Parliament for the use of living animals in scientific studies and in accordance with German law for the protection of animals. The protocol was approved by the Heinrich-Heine-University Animal Care Committee and by the district government of North-Rhine-Westphalia (LANUV; NRW; Permit Number 84-02.04.2015.A558; 81-02.04.2019.A270; 84-02.04.2017.A440). Experiments with human blood were reviewed and approved by the Ethics Committee of Heinrich-Heine-University. Subjects provided informed consent prior to their participation in the study (patients' consent). The experiments conform to the principles outlined in the Declaration of Helsinki.

Informed Consent Statement: Informed consent was obtained from all subjects involved in the study.

Data Availability Statement: The data presented in this study are available upon request from the corresponding author. The data are not publicly available due to [data size].

Acknowledgments: The authors would like to thank Martina Spelleken, Elena Schickentanz-Dey, and Meike Klier for the excellent performance of the experiments. We would like to acknowledge the Center for Advanced Imaging (CAi) at Heinrich-Heine-University Düsseldorf for providing access to the confocal microscope from Zeiss (LSM 880 Airyscan).

Conflicts of Interest: The authors declare no conflicts of interest.

References

1. Anversa, P.; Cheng, W.; Liu, Y.; Leri, A.; Redaelli, G.; Kajstura, J. Apoptosis and myocardial infarction. *Basic Res. Cardiol.* **1998**, *93* (Suppl. S3), 8–12. [CrossRef] [PubMed]
2. Jose Corbalan, J.; Vatner, D.E.; Vatner, S.F. Myocardial apoptosis in heart disease: Does the emperor have clothes? *Basic Res. Cardiol.* **2016**, *111*, 31. [CrossRef] [PubMed]
3. Abbate, A.; Bussani, R.; Amin, M.S.; Vetrovec, G.W.; Baldi, A. Acute myocardial infarction and heart failure: Role of apoptosis. *Int. J. Biochem. Cell Biol.* **2006**, *38*, 1834–1840. [CrossRef]
4. Green, D.R.; Llambi, F. Cell Death Signaling. *Cold Spring Harb. Perspect. Biol.* **2015**, *7*, a006080. [CrossRef] [PubMed]
5. Elmore, S. Apoptosis: A review of programmed cell death. *Toxicol. Pathol.* **2007**, *35*, 495–516. [CrossRef] [PubMed]
6. Hofstra, L.; Liem, I.H.; Dumont, E.A.; Boersma, H.H.; van Heerde, W.L.; Doevendans, P.A.; De Muinck, E.; Wellens, H.J.; Kemerink, G.J.; Reutelingsperger, C.P.; et al. Visualisation of cell death in vivo in patients with acute myocardial infarction. *Lancet* **2000**, *356*, 209–212. [CrossRef]
7. Abbate, A.; Biondi-Zoccai, G.G.; Baldi, A. Pathophysiologic role of myocardial apoptosis in post-infarction left ventricular remodeling. *J. Cell. Physiol.* **2002**, *193*, 145–153. [CrossRef]
8. Davidson, S.M.; Adameová, A.; Barile, L.; Cabrera-Fuentes, H.A.; Lazou, A.; Pagliaro, P.; Stensløkken, K.O.; Garcia-Dorado, D. Mitochondrial and mitochondrial-independent pathways of myocardial cell death during ischaemia and reperfusion injury. *J. Cell. Mol. Med.* **2020**, *24*, 3795–3806. [CrossRef]
9. Kajstura, J.; Cheng, W.; Reiss, K.; Clark, W.A.; Sonnenblick, E.H.; Krajewski, S.; Reed, J.C.; Olivetti, G.; Anversa, P. Apoptotic and necrotic myocyte cell deaths are independent contributing variables of infarct size in rats. *Lab. Investig.* **1996**, *74*, 86–107. [PubMed]
10. McCully, J.D.; Wakiyama, H.; Hsieh, Y.J.; Jones, M.; Levitsky, S. Differential contribution of necrosis and apoptosis in myocardial ischemia-reperfusion injury. *Am. J. Physiol. Heart Circ. Physiol.* **2004**, *286*, H1923–H1935. [CrossRef] [PubMed]
11. Holly, T.A.; Drincic, A.; Byun, Y.; Nakamura, S.; Harris, K.; Klocke, F.J.; Cryns, V.L. Caspase inhibition reduces myocyte cell death induced by myocardial ischemia and reperfusion in vivo. *J. Mol. Cell. Cardiol.* **1999**, *31*, 1709–1715. [CrossRef] [PubMed]
12. Schanze, N.; Bode, C.; Duerschmied, D. Platelet Contributions to Myocardial Ischemia/Reperfusion Injury. *Front. Immunol.* **2019**, *10*, 1260. [CrossRef] [PubMed]
13. Ibanez, B.; James, S.; Agewall, S.; Antunes, M.J.; Bucciarelli-Ducci, C.; Bueno, H.; Caforio, A.L.P.; Crea, F.; Goudevenos, J.A.; Halvorsen, S.; et al. 2017 ESC Guidelines for the management of acute myocardial infarction in patients presenting with ST-segment elevation: The Task Force for the management of acute myocardial infarction in patients presenting with ST-segment elevation of the European Society of Cardiology (ESC). *Eur. Heart J.* **2018**, *39*, 119–177. [CrossRef] [PubMed]

14. Ndrepepa, G.; Alger, P.; Kufner, S.; Mehilli, J.; Schömig, A.; Kastrati, A. ST-segment resolution after primary percutaneous coronary intervention in patients with acute ST-segment elevation myocardial infarction. *Cardiol. J.* **2012**, *19*, 61–69. [CrossRef] [PubMed]
15. Davis, M.; Movahed, M.R.; Hashemzadeh, M.; Hashemzadeh, M. The presence of idiopathic thrombocytopenic purpura correlates with lower rate of acute ST-elevation myocardial infarction. *Future Cardiol.* **2021**, *17*, 1327–1333. [CrossRef] [PubMed]
16. Fruchter, O.; Blich, M.; Jacob, G. Fatal acute myocardial infarction during severe thrombocytopenia in a patient with idiopathic thrombocytopenic purpura. *Am. J. Med. Sci.* **2002**, *323*, 279–280. [CrossRef] [PubMed]
17. Kolpakov, M.A.; Rafiq, K.; Guo, X.; Hooshdaran, B.; Wang, T.; Vlasenko, L.; Bashkirova, Y.V.; Zhang, X.; Chen, X.; Iftikhar, S.; et al. Protease-activated receptor 4 deficiency offers cardioprotection after acute ischemia reperfusion injury. *J. Mol. Cell. Cardiol.* **2016**, *90*, 21–29. [CrossRef] [PubMed]
18. Reusswig, F.; Dille, M.; Krüger, E.; Ortscheid, J.; Feige, T.; Gorressen, S.; Fischer, J.W.; Elvers, M. Platelets modulate cardiac remodeling via the collagen receptor GPVI after acute myocardial infarction. *Front. Immunol.* **2023**, *14*, 1275788. [CrossRef] [PubMed]
19. Reusswig, F.; Polzin, A.; Klier, M.; Dille, M.A.; Ayhan, A.; Benkhoff, M.; Lersch, C.; Prinz, A.; Gorressen, S.; Fischer, J.W.; et al. Only Acute but Not Chronic Thrombocytopenia Protects Mice against Left Ventricular Dysfunction after Acute Myocardial Infarction. *Cells* **2022**, *11*, 3500. [CrossRef] [PubMed]
20. Rubinfeld, G.D.; Smilowitz, N.R.; Berger, J.S.; Newman, J.D. Association of Thrombocytopenia, Revascularization, and In-Hospital Outcomes in Patients with Acute Myocardial Infarction. *Am. J. Med.* **2019**, *132*, 942–948.e945. [CrossRef] [PubMed]
21. Schönberger, T.; Ziegler, M.; Borst, O.; Konrad, I.; Nieswandt, B.; Massberg, S.; Ochmann, C.; Jürgens, T.; Seizer, P.; Langer, H.; et al. The dimeric platelet collagen receptor GPVI-Fc reduces platelet adhesion to activated endothelium and preserves myocardial function after transient ischemia in mice. *Am. J. Physiol. Cell Physiol.* **2012**, *303*, C757–C766. [CrossRef]
22. Xu, Y.; Huo, Y.; Toufektsian, M.C.; Ramos, S.I.; Ma, Y.; Tejani, A.D.; French, B.A.; Yang, Z. Activated platelets contribute importantly to myocardial reperfusion injury. *Am. J. Physiol. Heart Circ. Physiol.* **2006**, *290*, H692–H699. [CrossRef] [PubMed]
23. Schleicher, R.I.; Reichenbach, F.; Kraft, P.; Kumar, A.; Lescan, M.; Todt, F.; Göbel, K.; Hilgendorf, I.; Geisler, T.; Bauer, A.; et al. Platelets induce apoptosis via membrane-bound FasL. *Blood* **2015**, *126*, 1483–1493. [CrossRef]
24. Alexander, W.S.; Roberts, A.W.; Nicola, N.A.; Li, R.; Metcalf, D. Deficiencies in progenitor cells of multiple hematopoietic lineages and defective megakaryocytopoiesis in mice lacking the thrombopoietic receptor c-Mpl. *Blood* **1996**, *87*, 2162–2170. [CrossRef] [PubMed]
25. Gorressen, S.; Stern, M.; van de Sandt, A.M.; Cortese-Krott, M.M.; Ohlig, J.; Rassaf, T.; Gödecke, A.; Fischer, J.W.; Heusch, G.; Merx, M.W.; et al. Circulating NOS3 modulates left ventricular remodeling following reperfused myocardial infarction. *PLoS ONE* **2015**, *10*, e0120961. [CrossRef] [PubMed]
26. Heusch, G. Myocardial ischaemia-reperfusion injury and cardioprotection in perspective. *Nat. Rev. Cardiol.* **2020**, *17*, 773–789. [CrossRef] [PubMed]
27. Baldi, A.; Abbate, A.; Bussani, R.; Patti, G.; Melfi, R.; Angelini, A.; Dobrina, A.; Rossiello, R.; Silvestri, F.; Baldi, F.; et al. Apoptosis and post-infarction left ventricular remodeling. *J. Mol. Cell. Cardiol.* **2002**, *34*, 165–174. [CrossRef] [PubMed]
28. Xia, P.; Liu, Y.; Cheng, Z. Signaling Pathways in Cardiac Myocyte Apoptosis. *BioMed Res. Int.* **2016**, *2016*, 9583268. [CrossRef] [PubMed]
29. Cavalcante, G.C.; Schaan, A.P.; Cabral, G.F.; Santana-da-Silva, M.N.; Pinto, P.; Vidal, A.F.; Ribeiro-Dos-Santos, Â. A Cell's Fate: An Overview of the Molecular Biology and Genetics of Apoptosis. *Int. J. Mol. Sci.* **2019**, *20*, 4133. [CrossRef] [PubMed]
30. LA, O.R.; Tai, L.; Lee, L.; Kruse, E.A.; Grabow, S.; Fairlie, W.D.; Haynes, N.M.; Tarlinton, D.M.; Zhang, J.G.; Belz, G.T.; et al. Membrane-bound Fas ligand only is essential for Fas-induced apoptosis. *Nature* **2009**, *461*, 659–663. [CrossRef] [PubMed]
31. Tanaka, M.; Itai, T.; Adachi, M.; Nagata, S. Downregulation of Fas ligand by shedding. *Nat. Med.* **1998**, *4*, 31–36. [CrossRef] [PubMed]
32. Klatt, C.; Krüger, I.; Zey, S.; Krott, K.J.; Spelleken, M.; Gowert, N.S.; Oberhuber, A.; Pfaff, L.; Lückstädt, W.; Jurk, K.; et al. Platelet-RBC interaction mediated by FasL/FasR induces procoagulant activity important for thrombosis. *J. Clin. Investig.* **2018**, *128*, 3906–3925. [CrossRef] [PubMed]
33. Fliss, H.; Gattinger, D. Apoptosis in ischemic and reperfused rat myocardium. *Circ. Res.* **1996**, *79*, 949–956. [CrossRef] [PubMed]
34. Saraste, A.; Pulkki, K.; Kallajoki, M.; Henriksen, K.; Parvinen, M.; Voipio-Pulkki, L.M. Apoptosis in human acute myocardial infarction. *Circulation* **1997**, *95*, 320–323. [CrossRef] [PubMed]
35. Sanchis, D.; Llovera, M.; Ballester, M.; Comella, J.X. An alternative view of apoptosis in heart development and disease. *Cardiovasc. Res.* **2008**, *77*, 448–451. [CrossRef]
36. Inserte, J.; Cardona, M.; Poncelas-Nozal, M.; Hernando, V.; Vilardosa, Ú.; Aluja, D.; Parra, V.M.; Sanchis, D.; Garcia-Dorado, D. Studies on the role of apoptosis after transient myocardial ischemia: Genetic deletion of the executioner caspases-3 and -7 does not limit infarct size and ventricular remodeling. *Basic. Res. Cardiol.* **2016**, *111*, 18. [CrossRef] [PubMed]
37. Condorelli, G.; Roncarati, R.; Ross, J., Jr.; Pisani, A.; Stassi, G.; Todaro, M.; Trocha, S.; Drusco, A.; Gu, Y.; Russo, M.A.; et al. Heart-targeted overexpression of caspase3 in mice increases infarct size and depresses cardiac function. *Proc. Natl. Acad. Sci. USA* **2001**, *98*, 9977–9982. [CrossRef] [PubMed]
38. Boisguérin, P.; Covinhes, A.; Gallot, L.; Barrère, C.; Vincent, A.; Busson, M.; Piot, C.; Nargeot, J.; Lebleu, B.; Barrère-Lemaire, S. A novel therapeutic peptide targeting myocardial reperfusion injury. *Cardiovasc. Res.* **2020**, *116*, 633–644. [CrossRef] [PubMed]

39. Tanaka, M.; Ito, H.; Adachi, S.; Akimoto, H.; Nishikawa, T.; Kasajima, T.; Marumo, F.; Hiroe, M. Hypoxia induces apoptosis with enhanced expression of Fas antigen messenger RNA in cultured neonatal rat cardiomyocytes. *Circ. Res.* **1994**, *75*, 426–433. [CrossRef] [PubMed]
40. Yaniv, G.; Shilkrut, M.; Lotan, R.; Berke, G.; Larisch, S.; Binah, O. Hypoxia predisposes neonatal rat ventricular myocytes to apoptosis induced by activation of the Fas (CD95/Apo-1) receptor: Fas activation and apoptosis in hypoxic myocytes. *Cardiovasc. Res.* **2002**, *54*, 611–623. [CrossRef] [PubMed]
41. Lutz, A.; Sanwald, J.; Thomas, M.; Feuer, R.; Sawodny, O.; Ederer, M.; Borner, C.; Humar, M.; Merfort, I. Interleukin-1β enhances FasL-induced caspase-3/-7 activity without increasing apoptosis in primary mouse hepatocytes. *PLoS ONE* **2014**, *9*, e115603. [CrossRef] [PubMed]
42. Crist, S.A.; Elzey, B.D.; Ludwig, A.T.; Griffith, T.S.; Staack, J.B.; Lentz, S.R.; Ratliff, T.L. Expression of TNF-related apoptosis-inducing ligand (TRAIL) in megakaryocytes and platelets. *Exp. Hematol.* **2004**, *32*, 1073–1081. [CrossRef] [PubMed]
43. Meyer, T.; Amaya, M.; Desai, H.; Robles-Carrillo, L.; Hatfield, M.; Francis, J.L.; Amirkhosravi, A. Human platelets contain and release TWEAK. *Platelets* **2010**, *21*, 571–574. [CrossRef] [PubMed]
44. Otterdal, K.; Smith, C.; Oie, E.; Pedersen, T.M.; Yndestad, A.; Stang, E.; Endresen, K.; Solum, N.O.; Aukrust, P.; Damås, J.K. Platelet-derived LIGHT induces inflammatory responses in endothelial cells and monocytes. *Blood* **2006**, *108*, 928–935. [CrossRef] [PubMed]
45. Ong, S.B.; Samangouei, P.; Kalkhoran, S.B.; Hausenloy, D.J. The mitochondrial permeability transition pore and its role in myocardial ischemia reperfusion injury. *J. Mol. Cell. Cardiol.* **2015**, *78*, 23–34. [CrossRef] [PubMed]
46. Hohlbaum, A.M.; Moe, S.; Marshak-Rothstein, A. Opposing effects of transmembrane and soluble Fas ligand expression on inflammation and tumor cell survival. *J. Exp. Med.* **2000**, *191*, 1209–1220. [CrossRef] [PubMed]